Aging and nonlinear rheology in suspensions of polyethylene oxide–protected silica particles

Caroline Derec,[1,*] Guylaine Ducouret,[2] Armand Ajdari,[1] and François Lequeux[2]
[1]*Physico-Chimie Théorique, UMR CNRS-ESPCI 7083, ESPCI, 10 rue Vauquelin, 75231 Paris Cedex 5, France*
[2]*Physico-Chimie Macromoléculaire, UMR CNRS-ESPCI 7615, ESPCI, 10 rue Vauquelin, 75231 Paris Cedex 5, France*
(Received 2 December 2002; published 23 June 2003)

In an attempt to establish connections between classical rheology and aging in paste colloidal suspensions, we report in this paper a large set of experimental results on a given system. We have studied suspensions of polyethylene oxide–protected silica particles and performed classical rheology experiments that exhibit a very nonlinear behavior. We have then evidenced aging through stress relaxation as observed in various glassy systems, and finally show other manifestations of aging through various rheological experiments. Qualitative agreement between these experimental results and the predictions of a simple model suggests that the behavior observed experimentally is governed by the competition between aging and mechanically induced rejuvenation.

DOI: 10.1103/PhysRevE.67.061403 PACS number(s): 83.80.Hj, 83.10.Gr, 83.60.Df, 83.60.Pq

I. INTRODUCTION

Suspensions of soft repulsive particles display a very unusual ''paste'' behavior when concentrated beyond a critical value: they behave as an elastic solid under a weak mechanical perturbation, but flow under a larger one. They moreover display slow aging, which raised the question of their analogy with glassy systems. Experimentally, their nonlinear behavior and their slow relaxation make such systems very difficult to characterize in a clean way.

In the last few years, this analogy between glasses and concentrated soft systems has stimulated an important activity. Experimentally, similar features observed in extremely different systems have been pointed out. Aging phenomena have been studied by light scattering experiments in gels [1–5], foams [6], and repulsive colloidal suspensions [7]. Following the work of Struik [8] with amorphous polymers, rheological experiments have been performed on repulsive colloidal suspensions [9,10], or combined with diffusing wave spectroscopy [11].

In parallel, an important theoretical activity led to the development of several models based on different physical mechanisms. Models derived from Bouchaud's trap model were proposed to account for the rheology of such paste systems [12–14]. Other were proposed following the mode-coupling approach [15] and including the description of the effects of shear [16–18]. Phenomenological nonlinear models were also proposed [19–21], aiming at simpler analysis.

In this paper, we present an extended set of experimental results on suspensions of soft repulsive colloidal spheres. In Sec. II, we detail the outcome of the experiments performed on suspensions of polyethylene oxide–protected silica particles. The nonlinear mechanical properties of these suspensions are first characterized by classical rheology experiments. Then, we show that mechanical aging can be evidenced by different rheological experiments. The aim of this experimental part is to study various data to help in understanding the interplay between nonlinear rheology and slow dynamics. In Sec. III the predictions of a simple model that we have developed for the rheology near the fluid-paste transition [21] are confronted to the experimental results, in order to investigate whether its simple ingredients are sufficient to account for the complex rheology of paste systems observed.

II. EXPERIMENTAL RESULTS

A. Experimental system

Experiments are carried out with suspensions of silica particles stabilized by a layer of adsorbed polymer, prepared as described in Refs. [22,23]. The silica particles, commercialized by Nissan Chemical Ltd., have a diameter of about 100 nm. A dilute suspension is first washed in MilliQ$^+$ water by ultrafiltration until its conductivity becomes smaller than 10 μS/cm. Its salinity is then increased to $I=1.4\times10^{-2}M$, so that its Debye length is about 3 nm. The suspension is further stabilized by adsorption of a layer of polyethylen oxide (PEO) from Fluka of mass 5000 g/mol. The thickness of the PEO coating has been estimated to be of the order 7 nm [22]. Both steric and electrostatic repulsions ensure stability to the system.

Rheological measurements are performed on a strain controlled rheometer Rheometrics RFS II equipped with cone-plate geometry (diameter 50 mm, angle 2°, truncation 45 μm). To avoid drying of the sample, the geometry is immersed in silicone oil.

Many of the experiments described in the following are extremely sensitive to noise, particularly the ones with a ''waiting time,'' during which the suspension relaxes on its own with no mechanical perturbation. Most of these experiments are thus performed at night, and with the temperature regulator turned off, in order to get reproducible results.

B. Classical rheology

1. Steady-state flow curves

To characterize the system, we first perform steady-state rheology. The system is submitted to a constant shear rate $\dot{\gamma}$

*Present address: PMMH, UMR CNRS-ESPCI 7636. Email address: derec@pmmh.espci.fr

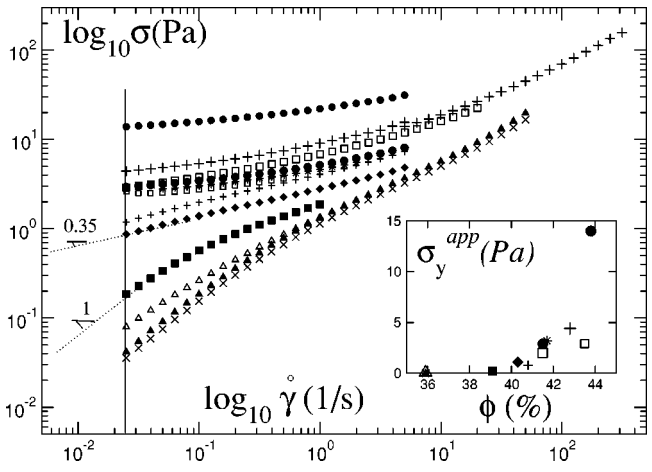

FIG. 1. Flow curves (log-log plot): steady-state shear stress versus shear rate for suspensions with various concentrations between 36% and 44% (from bottom to top). Dotted lines are guides for the eye. We define the apparent yield stress σ_y^{app} as the value of the stress for $\dot{\gamma}=0.025\ s^{-1}$ (vertical line). Inset: σ_y^{app} against volumic fraction ϕ.

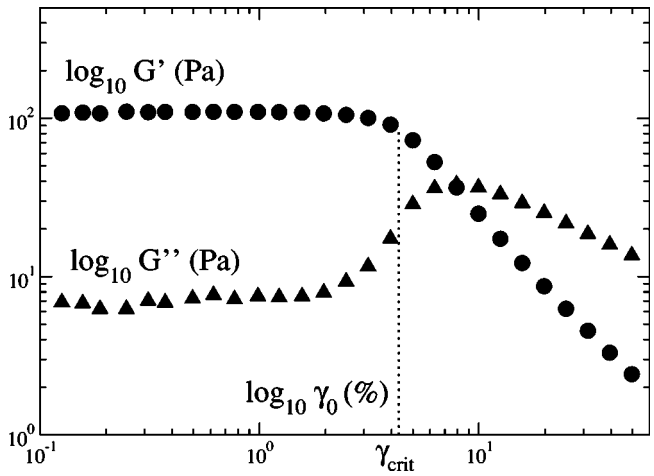

FIG. 2. Log-log plot of the elastic and loss moduli G' and G'' versus the amplitude γ_0 of the oscillatory shear at a frequency 1 Hz. At low deformation, the system behaves as an elastic linear solid. At high deformation, it exhibits a highly shear-thinning behavior. This sample has a yield stress $\sigma_y^{app}=3.2$ Pa.

and the corresponding shear stress σ is measured. Results are shown in Fig. 1 for suspensions of various concentrations from 36% to 44%. At low shear one can distinguish two types of behaviors: at low concentration the stress σ tends toward zero proportionally with $\dot{\gamma}$ and the system is Newtonian, whereas at high concentration the stress seems to tend to a finite value, the ''yield stress'' σ_y. Actually it is not clear whether the stress tends to a finite value or decreases very slowly. We thus arbitrarily define the *apparent* yield stress σ_y^{app} as the value of the stress for $\dot{\gamma}=0.025\ s^{-1}$ (limit value for the rheometer). In the inset σ_y^{app} is plotted against volumic fraction ϕ. As can be deduced from Fig. 1 and the inset, we can distinguish two very different behaviors: for $\phi \lesssim 40\%$ (liquid phase) the system is Newtonian and the apparent yield stress is very small ($\leqslant 0.2$ Pa), whereas for $\phi \gtrsim 40\%$ (''paste phase'') there is a weak or zero slope, and the apparent yield stress σ_y^{app} is about a few pascals and increases with concentration. For $\phi \simeq 40\%$, the stress varies roughly as $\dot{\gamma}^{0.35}$ when $\dot{\gamma}$ tends toward zero.

We now focus on systems in the paste phase, characterized by their apparent yield stress σ_y^{app} of a few pascals (which we will consistently use as an indirect measure of the concentration of a sample, given the difficulty and imprecision in obtaining ϕ).

2. Oscillatory rheology

The system is submitted to an oscillatory shear: $\gamma(t)=\gamma_0\cos(\omega t)$ and we measure the elastic and loss moduli G' and G''. Actually, we measure here the *effective* moduli, defined as the ratios of the first harmonics of the stress to the applied strain amplitude. Typical curves of G' and G'' versus the amplitude γ_0 are shown in Fig. 2 at a frequency $\omega/2\pi=1$ Hz. At very low deformations, G' is more than ten times larger than G'', and both are constant: the system behaves essentially as a linear elastic solid. For γ_0 larger than 2%, G'' increases roughly as $\gamma_0^{1.5}$, and the system behaves as a fluid at higher deformation. We found for all samples that the downward slope of G' at $\gamma_0>10\%$ is about twice the one of G'', and varies as $G' \propto \gamma_0^{-1.6\pm0.3}$.

Varying σ_y^{app} from 0.2 to 14 Pa (i.e., increasing concentration), the elastic modulus in the linear regime increases as $G' \sim 50\,\sigma_y^{app}$. The critical value γ_{crit} of the deformation between the linear and nonlinear regimes is about 4.5% whatever the yield stress of the sample. The corresponding critical value for the stress $\sigma_{crit}=G'/\gamma_{crit}$ is thus proportional to σ_y^{app}.

These values depend very weakly on the frequency $\omega/2\pi$ of the perturbation.

We now consider the viscoelastic moduli as a function of the frequency of the perturbation for a fixed amplitude in the linear regime ($\gamma_0=1\%$) (see Fig. 3). The elastic modulus is almost constant over three decades of frequency. The loss modulus displays a shallow minimum at a frequency of about 1 Hz, and then increases as $G'' \propto \omega^{0.5}$.

C. Mechanical aging

1. Stress relaxation

As mentioned in the Introduction, the analogy between paste and glassy phases leads us to expect aging features in concentrated silica suspensions. In an earlier paper [9], we proposed a procedure to measure aging in colloidal systems. We first apply a *mechanical fluidification* to put the system in a history-independent fluidified state. This fluidification has been empirically determined to get reproducible subsequent mechanical responses: the sample is submitted to an oscillatory shear of amplitude 1000% at 1 Hz during 200 s. When fluidification is stopped at $t=0$, the system evolves spontaneously during a time t_w, classically called the waiting time. At $t=t_w$, a small deformation γ_m (in the linear regime) is applied, and the relaxation of the stress $\sigma(t)$ is measured as a function of the elapsed time $t'=t-t_w$.

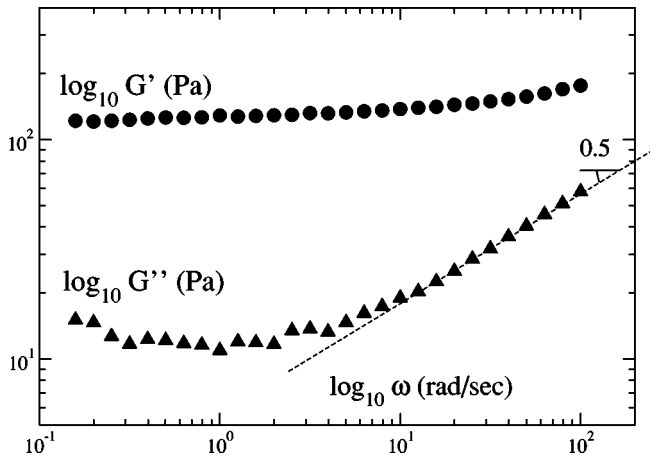

FIG. 3. Log-log plot of the elastic and loss moduli under oscillatory shear at fixed amplitude $\gamma_0=1\%$ and variable frequency. The elastic modulus is almost constant, and the loss modulus G'' exhibits a shallow minimum around 1 Hz, and a power-law dependence at high frequency: $G''\propto\omega^{0.5}$. This sample has a yield stress $\sigma_y^{app}=4.3$ Pa.

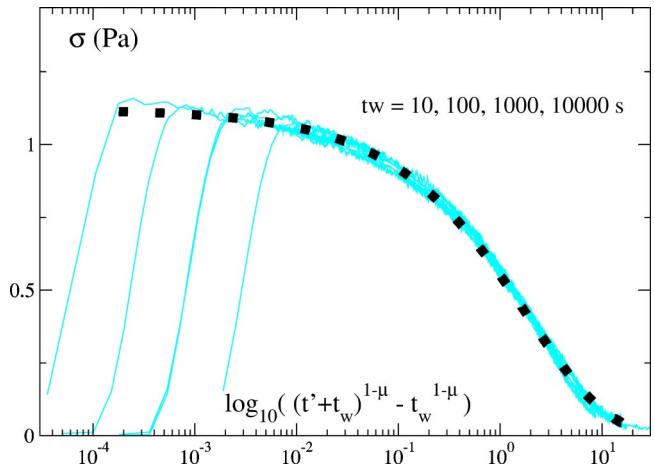

FIG. 4. Semilogarithmic plot of the stress relaxation against $(t'+t_w)^{1-\mu}-t_w^{1-\mu}$, with $\mu=0.55$. The sample ($\sigma_y^{app}=3.2$ Pa) was submitted to a step strain $\gamma_m=1\%$ at $t'=0$, after different values of the waiting time: $t_w=10$, 100, 1000, 10 000 s. Big dots: fit from Eq. (1) with $\gamma_m=1\%$, $G=112$ Pa, $\tau=4s$, $\beta=0.55$, and $\mu=0.55$.

The stress relaxation depends strongly on the waiting time t_w: the larger the waiting time, the slower the relaxation. There is thus seemingly no intrinsic relaxation time in our system. Furthermore, we have found that, for a given sample, curves for different waiting times collapse when plotted against a rescaled expression of time: $(t'+t_w)^{1-\mu}-t_w^{1-\mu}$ (Fig. 4). The exponent μ, classically called the aging exponent [8,24], is found to be 0.7 ± 0.2 for different samples. This value seems to be uncorrelated to the value of the yield stress (for $2<\sigma_y^{app}<6$ Pa) or to the amplitude of the perturbation (for $0.2\%<\gamma_m<2\%$) [25]. The rescaled curves are well fitted by a stretched exponential (see Fig. 4):

$$\sigma=G\gamma_m\exp\left[-\left(\frac{(t'+t_w)^{1-\mu}-t_w^{1-\mu}}{\tau^{1-\mu}}\right)^{\beta}\right], \qquad (1)$$

with $0.50<\beta<0.68$ and $3.9<\tau<7.4$ s for the different samples tested ($2<\sigma_y^{app}<6$ Pa).

Let us remark that the maximum value of the stress divided by the applied strain is a measure of the high-frequency elastic modulus (as the system at small times responds elastically to the deformation ramp that brings γ from 0 to γ_m in a time ~0.1 s). It is obvious in Fig. 4 that this maximum stress depends on the waiting time t_w. Plotting experimental values suggests roughly a logarithmic increase, but this increase can also be reasonably fitted by expression (1) with a fixed value of $t'=0.1$ s (ramp time).

2. Slow drift of the elastic modulus

To test this possible weak time dependence of the elastic modulus, we used the following procedure: fluidification, spontaneous evolution during t_w, and application at $t'=t-t_w=0$ of an oscillatory shear at frequency 1 Hz and of amplitude $\gamma_0=1\%$ (linear regime). For $t'>0$, the evolution of the elastic modulus G' is measured after different values of the waiting time. We found that the elastic modulus G' increases with time. In fact, this increase does not depend on t_w but on the time t elapsed since the end of the fluidification (i.e., the measure does not perturb the intrinsic increase of G'). When plotted against t (Fig. 5), all curves tend to increase logarithmically. Varying concentration, we found typically

$$G'\sim G_0+a\log_{10}(t), \qquad (2)$$

with a comparable to σ_y^{app}. For small amplitude γ_0 of the applied oscillatory shear, the slope a is constant, but it decreases with γ_0 when $\gamma_0\geqslant3\%$. Thus, beyond the linear regime, mechanics prevents the aging of the elastic modulus.

This logarithmic increase of G' is comparable with the increase of the high-frequency elastic modulus as pointed in stress relaxation measurements and may be the manifestation of the same mechanism.

We have performed similar experiments on suspensions of the same silica particles but stabilized only by electrostatic repulsion (without polymer coating) [26]. We have observed the same logarithmic increase [Eq. (2)] for samples in a large range of concentrations ($3<\sigma_y^{app}<70$ Pa) with the slope a comparable to σ_y^{app}. Remarkably this logarithmic increase was also found in another system, a colloidal suspension of polyelectrolyte microgels [27]. These three suspensions (silica with or without PEO and polyelectrolyte microgels) display aging features as described in Sec. II C 1. This may indicate a link between aging in the stress relaxation and spontaneous logarithmic increase of the elastic modulus.

Note that this mild increase of G' has only a weak effect on the experiments under oscillatory shear reported in Figs. 2 and 3.

D. Start-up flow

Finally, we perform start-up flow experiments: after fluidification, the system evolves spontaneously during t_w, and

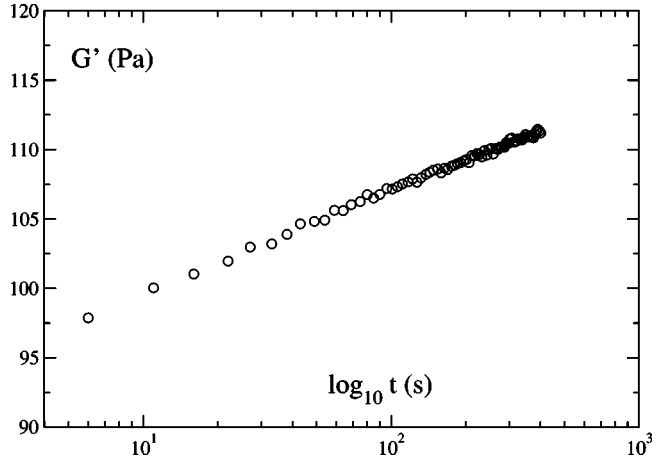

FIG. 5. Semilogarithmic plot of the elastic modulus versus t upon oscillatory shear of amplitude 1% at frequency 1 Hz, for a sample with $\sigma_y^{app}=2.9$ Pa.

the stress is then measured after the application of a constant shear rate $\dot{\gamma}$ from $t'=t-t_w=0$ on.

We first fix the waiting time t_w, and study the response as a function of the applied $\dot{\gamma}$. An example is given in Fig. 6 for $t_w=100$ s and various shear rates $0.1<\dot{\gamma}<10\ \mathrm{s}^{-1}$. In response to the application of shear, the stress σ first increases proportionally to the strain. It then overshoots to a critical value σ_{plas} that depends on $\dot{\gamma}$. When σ has reached σ_{plas} the system is forced to flow, and the stress relaxes to its steady-state value σ_{ss} that also depends on $\dot{\gamma}$ (see the flow curve in Fig. 1).

In Fig. 7 σ_{plas} is plotted against $\dot{\gamma}$ (full circles): it increases as $\dot{\gamma}^{0.27}$ over two decades of $\dot{\gamma}$. The increase of σ_{plas} may be understood as follows: the smaller $1/\dot{\gamma}$ compared to some intrinsic time characteristic of rearrangements in the system, the larger the stress stored before rearrangements occur.

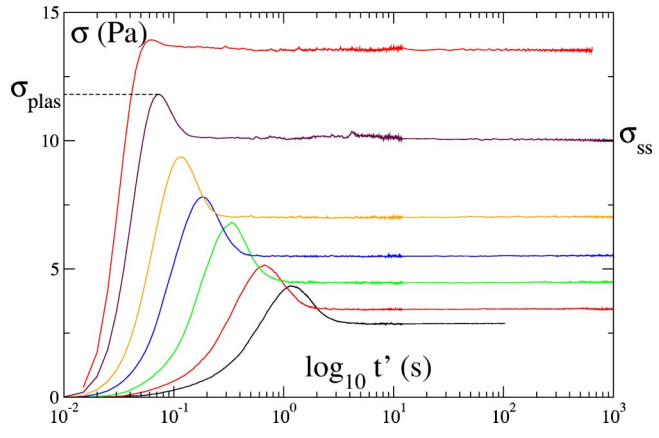

FIG. 6. Semilogarithmic plot of the stress σ versus t', after $t_w=100$ s, under various constant shear rates $0.1<\dot{\gamma}<10\ \mathrm{s}^{-1}$ (from right to left). The stress σ increases linearly until it reaches the critical value σ_{plas} depending on $\dot{\gamma}$, and then relaxes to the stationary value σ_{ss}. This sample has a yield stress $\sigma_y^{app}=2.5$ Pa.

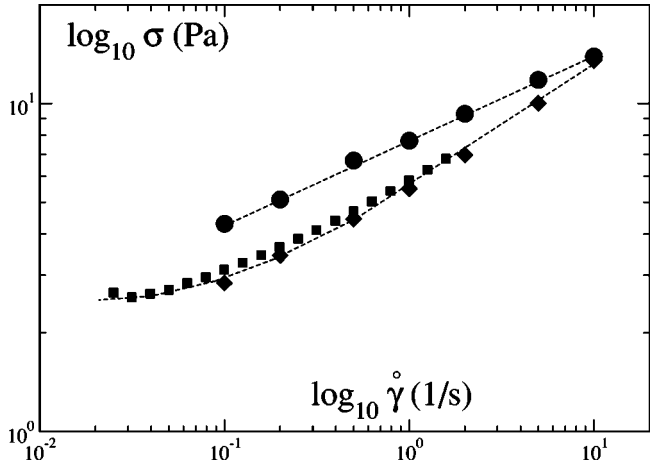

FIG. 7. Circles and diamonds: respectively, σ_{plas} and σ_{ss} from Fig. 6. Squares: steady-state flow curve for the same sample from other shear flow experiment. Dotted lines are guides for the eye (log-log plot).

We have also observed that the amplitude of the overshoot $(\sigma_{plas}-\sigma_{ss})$ tends to zero at very low and high shear rates.

Finally, we have tested the effects of aging on this transient regime, by applying to the sample the same shear rate after various waiting times. We found that at fixed $\dot{\gamma}$, the critical value σ_{plas} increases with the waiting time (Fig. 8): the older the sample, the more stress stored before flow occurs. However, the time at which first rearrangements occur seems to be constant, i.e., the deformation at which flow occurs does not depend on t_w.

Note that the amplitude of this increase of σ_{plas} as a function of the system age is comparable with the amplitude of the increase of the linear elastic modulus G' described in Sec. II C 2. We have, however, not gathered sufficient data to distinguish between a logarithmic and a weak power-law dependence.

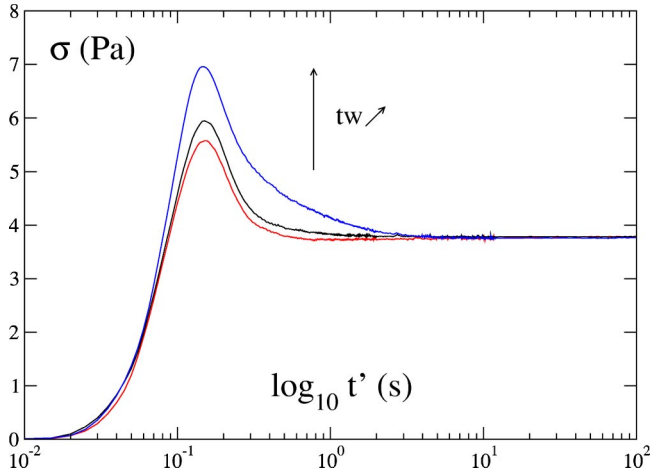

FIG. 8. Semilogarithmic plot of the stress versus t' under constant shear rate $\dot{\gamma}=1\,\mathrm{s}^{-1}$, after various values of the elapsed waiting time: $t_w=100$, 1000, 10 000 s. This sample has a yield stress $\sigma_y^{app}=1.5$ Pa.

E. Conclusion on the experiments

We have reported here a set of measurements for a given colloidal paste system, spanning both classical rheology and aging experiments. Features similar to those reported above for steady-state and oscillatory shear have already been observed individually in various pasty systems: colloidal suspensions [27,28], emulsions [29–32], or foams [33]. However. scarce are the papers where the complete set of results is given.

Let us emphasize again that aging experiments are quite difficult to perform, as they are extremely sensitive to external noise (e.g., experiments carried out at night were systematically more reproducible than those performed during the day), and a very accurate procedure must be followed to get reproducible results. In the last few years, several experiments have been performed to characterize aging in repulsive colloidal suspensions [9–11]. Despite their very different physicochemical properties, these systems exhibit analogous features, and, in particular, a similar dependence on age during spontaneous relaxation. The logarithmic increase of the elastic modulus has been observed in different systems too, but was not underlined as an other manifestation of aging in these paste systems. Finally, our start-up flow experiments show that this procedure may be a different and complementary way to probe aging. Until a clear link between these different manifestations of aging is established, we suggest that it should prove useful to record these various data.

III. CONFRONTATION WITH A SIMPLE MODEL

In this section, we confront the experimental results of Sec. II to the predictions of a simple model that we have developed for the rheological behavior near the fluid-paste transition [21]. We do not expect from such a simple model a complete and quantitative description of the rheological behavior of our concentrated suspensions. However, we will show that this model is able to capture many essential features of the extended set of experiments presented in preceding section.

We first briefly recall the model (see Ref. [21] for details), and then confront its predictions to the experiments.

A. The model

The two main physical ingredients in the model are spontaneous aging, on the one hand, and rejuvenation induced by mechanics, on the other hand. Even if it is now accepted that the dynamics in such systems may be governed by a spectra of relaxation times, we made for simplicity the choice of one characteristic time, that itself evolves with time, in the hope to describe by this minimal way the coupling between aging and nonlinear rheology.

The basic hypothesis is thus the following: the dynamics at low frequency is governed by one scalar variable D, the ''fluidity,'' that is the inverse of a mechanical relaxation time. The stress evolution is described by the equation

$$\partial_t \sigma = -D\sigma + G\dot{\gamma}, \tag{3}$$

where σ and $\dot{\gamma}$ are, respectively, the stress and the applied shear rate, and G is the elastic modulus, taken to be constant. The stress σ is rescaled so that G is fixed to 1. Equation (3) with a constant D is the usual Maxwell model for linear viscoelastic systems. In our model, in contrast, the fluidity is not constant but evolves with time.

In the vicinity of the fluid-paste transition, the characteristic time D^{-1} is always large. In the fluid phase this time is finite, whereas it tends to infinity in the paste phase. We thus propose the following expansion for the evolution of D: $\partial_t D = rD^{\alpha} - vD^{\alpha+\beta}$. The constant v is positive, whereas the parameter r is positive in the fluid phase and negative in the paste one (r is directly related to the difference between the experimental concentration ϕ and the ''critical'' one (about 40%) between fluid and paste phases. If we want the fluidity D to play the role of memory of the system, then $\alpha \geqslant 2$, so that D relaxes slower than the stress σ.

The second essential point is that application of a shear rate induces rearrangements in the system, so as to allow flow. We thus simply postulate that shear tends to increase the fluidity D and write $\partial_t D = rD^{\alpha} - vD^{\alpha+\beta} + f(\sigma, D, \dot{\gamma})$, with f a positive and regular function of σ, D, and $\dot{\gamma}$. We choose for simplicity f to be a power law in the three variables, which introduces three new exponents

$$\partial_t D = \left[r + u\left(\frac{\sigma D}{\dot{\gamma}}\right)^{\lambda} \frac{\dot{\gamma}^{\nu-\epsilon}}{D^{\nu}} \right] D^{\alpha} - vD^{\alpha+\beta}. \tag{4}$$

This somewhat awkward form for f emphasizes that the exponent λ is irrelevant at low frequencies (where $\sigma D = \dot{\gamma}$).

B. Confrontation to experiments

This simple model was built to describe the rheology near the fluid-paste transition, with the parameter r a measure of the distance to the transition. Within this model, the yield stress (or apparent yield stress), characteristic of the distance to the transition, varies as $\sigma_y \propto (-r)^{1/\nu}$, and the elastic modulus G is constant. In contrast, we found experimentally $G' \propto \sigma_y^{app}$. Our model is then clearly not able to describe variations of the rheological behavior with the distance to the transition, unless we make further assumptions as to the value of G.

We leave this aside and from now on try to confront the predictions of the model to the experiments in the paste phase for a fixed $r < 0$ (fixed $\sigma_y > 0$).

The model is limited to the description of the low-frequency or long-time behavior. To confront it to experiments, we artificially add a Maxwell high-frequency contribution: the total stress is the sum of σ [as given by Eq. (3)] and σ_0, where σ_0 obeys the following Maxwell equation $\partial_t \sigma_0 = -\sigma_0/\tau_0 + G_0\dot{\gamma}$, with τ_0 a constant short time.

1. Classical rheology

We will now consider successively the various experiments reported in Sec. II. We first probe the response of the system to an oscillatory shear: a deformation $\gamma(t) = \gamma_0 \cos(\omega t)$ is applied and the elastic and loss moduli G' and G'' are calculated (for details see Ref. [21]).

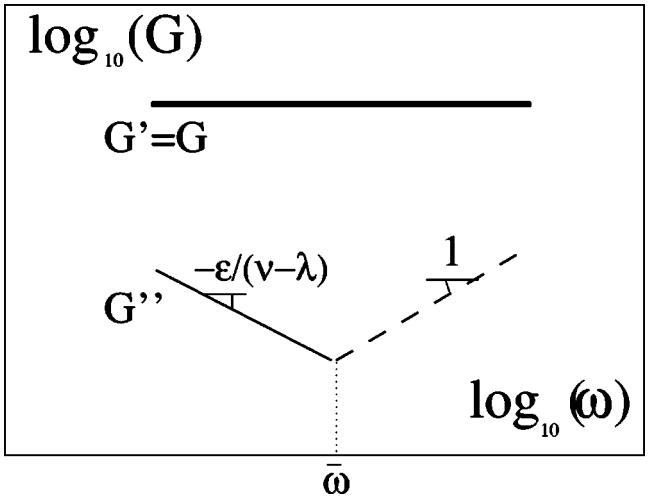

FIG. 9. Schematic log-log plot of the elastic and loss moduli G' and G'' against frequency, at a fixed strain amplitude γ_0. Full line: basic model [Eqs. (3) and (4)]. Dashed line: contribution of high-frequency term. G'' displays a minimum for $\omega=\bar{\omega} \sim \gamma_0^{(\nu-\epsilon)/(\nu+\epsilon-\lambda)}$.

Let us first describe the frequency dependence at a fixed small strain amplitude γ_0. Two characteristic modes appear: a fast one of characteristic time τ_0 (high-frequency contribution) and a slow non-linear one. We only represented in Fig. 9 the results for frequencies within the window separating these two values. The results are qualitatively in line with experiments (see Fig. 3): G' displays a plateau and G'' a minimum for $\omega=\bar{\omega}\sim \gamma_0^{(\nu-\epsilon)/(\nu+\epsilon-\lambda)}$.

We now turn to a variable strain amplitude γ_0 at a fixed frequency ω such that $\bar{\omega}<\omega<1/\tau_0$. Results, schematized in Fig. 10, are again qualitatively similar as in experiments (see Fig. 2). At low deformation, the response is elastic with a constant elastic modulus G', and with a viscous plateau due

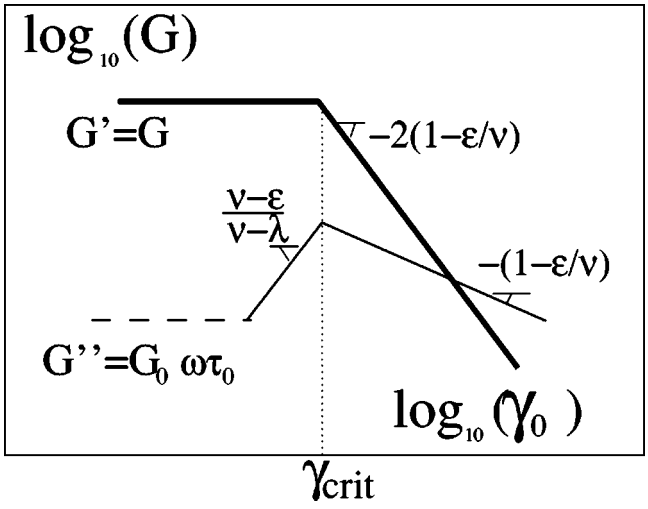

FIG. 10. Schematic log-log plot of the elastic and loss moduli G' and G'' against strain amplitude, at a fixed frequency $\bar{\omega}<\omega<1/\tau_0$. Full line: basic model [Eqs. (3) and (4)]. Dashed line: contribution of high-frequency term.

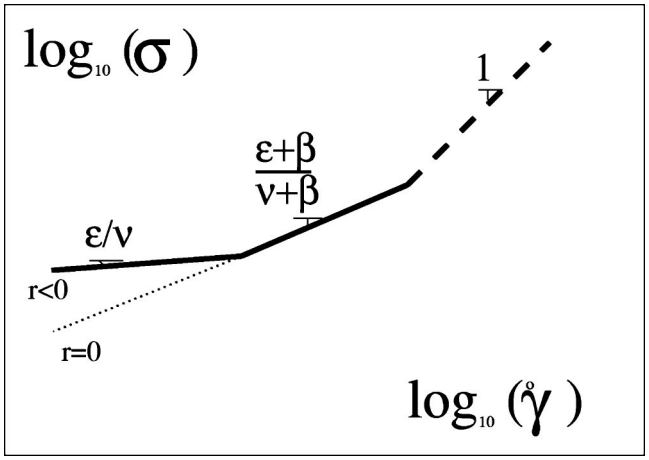

FIG. 11. Schematic flow curve (log-log plot): steady-state stress versus applied shear rate. Full line: basic model. Dashed line: contribution of high-frequency term. Dotted line: critical regime ($r=0$).

here to the high-frequency term. At high deformation the system is viscous, and the ratio of the slopes of G' and G'' equals 2, which is in good agreement with experimental results. Attempting a more quantitative comparison with experiments for the slopes gives $\epsilon/\nu\sim 0.20$ and $\lambda/\nu\sim 0.45$.

From Fig. 9, it is difficult to get for G'' a numerical value for the power-law dependence on ω at low frequency, as this decrease of G'' is at the limit of the experimental window. If we put in the model the numerical values obtained from Fig. 10 ($\epsilon/\nu\sim 0.20$, $\lambda/\nu\sim 0.45$), we get $G''\sim\omega^{-0.35}$, which is compatible with experimental observations.

Let us remark that the addition of the high-frequency term in the model allows to get curves whose shapes are similar to the experimental ones. It is, in particular, necessary to account for the existence of a viscous plateau at low deformation (Fig. 10) as observed experimentally. But this high-frequency term is qualitatively clearly incorrect at low deformation ($G''=G_0\omega\tau_0$) and high frequency ($G''\propto\omega$, whereas we found experimentally $G''\propto\omega^{0.5}$). The choice of a Maxwell element for the high-frequency contribution is clearly too simple.

Finally, we consider the predictions of the model for the flow curve, which is represented schematically in Fig. 11. At low shear rates, the stress σ varies as a power law of $\dot{\gamma}$: $\sigma=(-r/u)^{1/\nu}\dot{\gamma}^{\epsilon/\nu}$. At higher shear rates, where $vD^{\alpha+\beta} \gg rD^{\alpha}$ [see Eq. (4)], an other shear-thinning r-independent regime appears. At very high shear, the system becomes Newtonian because of our choice for the high-frequency term.

This flow curve is in qualitative agreement with experimental results (see Fig. 1). Our model indeed predicts anomalous power-law regimes at low and intermediate shear rates as the competition and equilibrium between spontaneous aging [term proportional to r in Eq. (4)] and mechanical rejuvenation (term proportional to u).

It is difficult to make the comparison more quantitative as extracting exponents from the curves of Fig. 1 is clearly somewhat arbitrary: the increase at low shear is very slow,

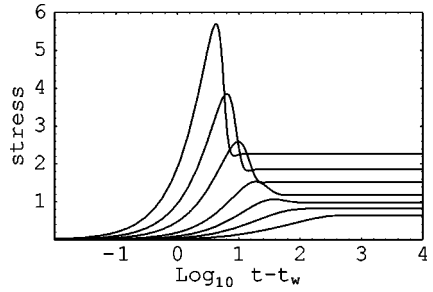

FIG. 12. Numerics with $\alpha=2.5$, $\beta=0.25$, $\epsilon=0.2$, $\nu=1$, $\lambda=0.45$, $-r=u=v=1$: Semilogarithmic plot of the stress σ versus t' with $(1/t_w)^{2/3}\propto D_{t_w}=0.1$ and $0.02<\dot{\gamma}<2$ from right to left.

implying large cross-over domains. If we use the numerical values obtained from the previous comparison (namely, $\epsilon/\nu \sim 0.2$), the model predicts: $\sigma\propto\dot{\gamma}^{0.2}$ at very low shear, which is compatible with experiments.

For the critical region ($r\sim 0$), the experiments suggest $\sigma(\phi\simeq 40\%)\sim\dot{\gamma}^{0.35}$, which leads to $\beta/\nu\sim 0.25$.

2. Aging in stress relaxation

We apply to the model the procedure of aging experiments: fluidification interrupted at $t=0$, spontaneous relaxation during t_w, and at $t'=t-t_w=0$ application of a small step strain in the linear regime. The influence of the preparation is wholly contained in the values of D and σ at time $t=0$ denoted by D_0 and σ_0.

For $t>0$, the fluidity relaxes to zero as $D(t)\propto 1/t^{\mu}$, where $\mu=1/(\alpha-1)$ plays the role of the aging exponent. This slow relaxation accounts for the very long memory of the system of its past history (initial conditions at time $t=0$). As soon as $t_w \gg D_0^{-1/\mu}\mu/|r|$, the stress relaxation after the step strain takes the form (for $\mu<1$)

$$\sigma\propto\exp\left(-(\mu/|r|)^{\mu}\frac{(t'+t_w)^{1-\mu}-t_w^{1-\mu}}{1-\mu}\right). \qquad (5)$$

Remarkably, the argument of the exponential is the function used to rescale our experimental data: $(t'+t_w)^{1-\mu}-t_w^{1-\mu}$ [see Eq. (1)] [34].

Comparison to experimental values of μ impose $2.1<\alpha<3$. Expression (5) exhibits a characteristic time proportional to $|r|^{\mu/1-\mu}$. Such a time appears formally in the rescaling used experimentally [see τ in Eq. (1)]. However, the simple exponential form is not compatible with the stretched exponential observed experimentally. This may be due to our choice of describing the dynamics by a single time $1/D$.

3. Start-up flow

Finally, we confront the model with start-up flow experiments. As the analytical resolution is more complex here, the prediction of the model is evaluated numerically.

After spontaneous evolution during t_w, a constant shear rate $\dot{\gamma}$ is applied at $t'=0$ and the corresponding stress is recorded. For large enough t_w, the initial conditions are given by $\sigma(t'=0)\sim 0$ and $D(t'=0)=D_{t_w}\propto(1/t_w)^{\mu}$.

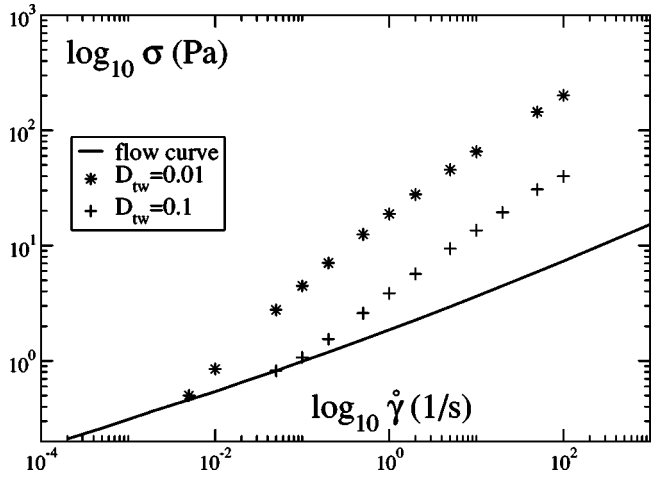

FIG. 13. Numerical results with the same parameter values as for Fig. 12. Symbols: log-log plot of σ_{plas} versus $\dot{\gamma}$ with $(1/t_w)^{2/3}\propto D_{t_w}=0.01$ and 0.1. Full line: flow curve.

We use for the exponents values compatible with the comparisons of Secs. III B 1 and III B 2 $\alpha=2.5$, $\beta/\nu=0.25$, $\epsilon/\nu=0.2$, $\lambda/\nu=0.45$, the exponent ν being still undetermined. An example of numerical result is plotted in Fig. 12 for $\nu=1$, $-r=u=v=1$, $D_{t_w}=0.1$, and different values of the applied shear rate $\dot{\gamma}$.

As observed in experiments, an overshoot is predicted: the stress first increases linearly up to the maximum value σ_{plas} and then relaxes to the steady-state value. The maximum value σ_{plas} is reached faster for larger $\dot{\gamma}$, and its value strongly depends on $\dot{\gamma}$ (see Fig. 13): σ_{plas} varies roughly as $\dot{\gamma}^{0.5}$. This power-law dependency is slightly larger than the one observed in experiments. At low shear, σ_{plas} meets the flow curve: no more overshoot appears.

We have checked numerically that this behavior is qualitatively the same for different values of ν.

We finally fix the value of the applied shear $\dot{\gamma}$ and test the dependence on the waiting time, or initial condition D_{t_w}. An example is given in Fig. 14 with the same numerical values as in Fig. 12, at fixed $\dot{\gamma}=0.1$ and varying D_{t_w}. As in experiments, the value of σ_{plas} increases with the waiting time. Note that this effect is not linked here to an increase of the elastic modulus as noted in experiments, as G is supposed

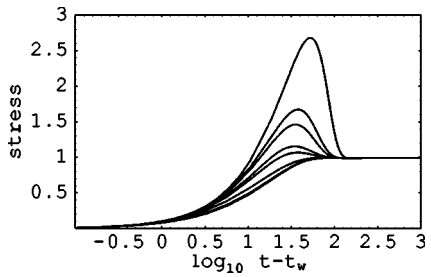

FIG. 14. Numerics with the same parameter values as for Fig. 12. Semilogarithmic plot of the stress σ versus t' with $\dot{\gamma}=0.1$ and different initial conditions: $0.02<D_{t_w}<2$ from top to bottom.

constant in the model. Contrary to experiments, the time (i.e., the deformation) at which flow occurs is not constant but smoothly drifts with the age.

C. Conclusion on the confrontation

This phenomenological model, which does not refer to any microscopic mechanism, relies on two main ingredients: spontaneous aging and rejuvenation induced by mechanics. We have shown that its predictions for classical rheology are in good qualitative agreement with the experimental results. More remarkable is the very simple description of aging, with the natural occurrence of the scaling variable that is the outcome of more sophisticated and complex theories [24], and that we used successfully to fit the data of our silica systems. Finally, the existence of an overshoot in start-up flows is described too, and its dependence on the age is well predicted. We have thus shown that this coupling between aging and mechanical rejuvenation is the right mechanism to qualitatively account for the rheology of paste systems.

However, from a quantitative point of view, it is difficult to determine the form of this coupling. We have seen that one can find a set of numerical values for the exponents that gives a good fit for the experiments. But because of the number of exponents involved, and because of the difficulty to get accurate slope values from experiments (large cross over domains), there are still undetermined exponents. In that sense, it is still very difficult to compare from a quantitative point of view these experiments on pasty systems with a model, even so simple. Moreover, our model is clearly unable to describe how the rheological behaviors in the paste phase depend on the distance to the fluid-paste transition. Furthermore, the choice of only one characteristic time is not sufficient to describe the complex dynamics of such systems, particularly the relaxation of the stress as a stretched exponential (or the slow evolution of the elastic modulus). However, in the absence of other analytically simple models, we consider that this model is a useful first-order guide for experiments.

IV. CONCLUSION

In this paper, we have presented a set of experimental results on a simple colloidal system (PEO-protected silica particles), including both classical rheology and aging experiments. These results have been confronted to the predictions of a simple model, in order to point out the basic ingredients necessary to account for these experiments.

Experimentally, classical rheological tests show the unusual mechanical responses characteristic of paste systems: nonlinearities at very low deformation, existence of a critical value of the stress that depends on the solicitation. The analogy between paste and glassy systems has been validated by the characterization of aging in these silica suspensions: the dynamics of the system depends on its ''age'' in a way similar to glassy systems, and we have proposed a procedure that takes this fact into account and rationalizes behaviors that seem *a priori* nonreproducible. Moreover, we have proposed a way to characterize aging through start-up flow experiments.

In parallel, we have recalled a model built on two basic ingredients: spontaneous aging and rejuvenation induced by mechanics. We have shown that this very simple approach is able to qualitatively describe many of the unusual behaviors observed in our paste systems; nonlinear rheology and aging through different experiments. However, even if we have been able to make some quantitative comparisons (mostly in terms of the exponents) between its predictions and the experimental results, this model in its present form is clearly not adapted as a quantitative guide for experiments, but remains qualitatively very satisfactory given its simplicity.

We have shown the strong interplay between nonlinear rheology and aging, and emphasized various mechanical manifestations of aging (through stress relaxation, start-up flow experiments, and increase of G'), between which the link is still to be understood. It would be interesting to perform a similar extended set of experiments on other colloidal systems, in order to assess or infirm the existence of universal features in paste systems.

[1] D. Bonn, H. Tanaka, G. Wegdam, H. Kellay, and J. Meunier, Europhys. Lett. **45**, 52 (1998).

[2] A. Knaebel, M. Bellour, J-P. Munch, V. Viasnoff, F. Lequeux, and J.L. Harden, Europhys. Lett. **52**, 73 (2000).

[3] L. Cipelletti, S. Manley, R.C. Ball, and D.A. Weitz, Phys. Rev. Lett. **84**, 2275 (2000).

[4] P.N. Segre, V. Prasad, A.B. Schofield, and D.A. Weitz, Phys. Rev. Lett. **86**, 6042 (2001).

[5] B. Abou, D. Bonn, and J. Meunier, Phys. Rev. E **64**, 021510 (2001).

[6] R. Höhler, S. Cohen-Addad, and A. Asnacios, Europhys. Lett. **48**, 93 (1999).

[7] V. Viasnoff and F. Lequeux, Phys. Rev. Lett. **89**, 065701 (2002).

[8] L.C.E. Struik, *Physical Aging in Amorphous Polymers and Other Materials* (Elsevier, Houston, 1978).

[9] C. Derec, A. Ajdari, G. Ducouret, and F. Lequeux, C. R. Acad. Sci. Paris **t.1,IV**, 1115 (2000).

[10] M. Cloître, R. Borrega, and L. Leibler, Phys. Rev. Lett. **85**, 4819 (2000).

[11] L. Ramos and L. Cipelletti, Phys. Rev. Lett. **87**, 245503 (2001).

[12] P. Sollich, F. Lequeux, P. Hebraud, and M.E. Cates, Phys. Rev. Lett. **78**, 2020 (1997).

[13] P. Sollich, Phys. Rev. E **58**, 738 (1998).

[14] S.M. Fielding, P. Sollich, and M.E. Cates, J. Rheol. **44**, 323 (2000).

[15] W. Götze, in *Liquids, Freezing and Glass Transition*, Proceedings of the Les Houches Summer School of Therotical Physics edited by J.P. Hansen, D. Levesque, and J. Zinn-Justin (North-Holland, Amsterdam, 1989), p. 403.

[16] L. Berthier, J.L. Barrat, and J. Kurchan, Phys. Rev. E **61**, 5464 (2000).

[17] M. Fuchs and M.E. Cates, Phys. Rev. Lett. **89**, 248304 (2002).

[18] M. Fuchs and M.E. Cates, e-print cond-mat/0207530.
[19] P. Hebraud and F. Lequeux, Phys. Rev. Lett. **81**, 2934 (1998).
[20] C. Derec, A. Ajdari, and F. Lequeux, Faraday Discuss. **112**, 195 (1999).
[21] C. Derec, A. Ajdari, and F. Lequeux Eur. Phys. J. E **4**, 355 (2001).
[22] O. Neel, Thèse de l'université Paris VI, 1995.
[23] O. Neel, G. Ducouret, and F. Lafuma, J. Colloid Interface Sci. **229**, 244 (2000).
[24] J.-P. Bouchaud, L.F. Cugliandolo, M. Mezard, and J. Kurchan, in *Spin Glasses and Random Fields*, edited by A.P. Young (World Scientific, Singapore, 1997).
[25] This result is in contrast with the one of Ref. [10] where, in creep experiments, a decrease of μ with the amplitude of the perturbation was found.
[26] C. Derec, thèse de l'Université Paris VII, 2001.
[27] R. Borrega, thèse de l'Université Paris VI, 2000.
[28] R.J. Ketz, R.K. Prud'homme, and W.W. Graessley, Rheol. Acta **27**, 531 (1988).
[29] T.G. Mason, J. Bibette, and D.A. Weitz, Phys. Rev. Lett. **75**, 2051 (1995).
[30] T.G. Mason, J. Bibette, and D.A. Weitz, J. Colloid Interface Sci. **179**, 439 (1996).
[31] P. Hebraud, F. Lequeux, and J.-F. Palierne, Langmuir **16**, 8296 (2000).
[32] A.J. Liu, S. Ramaswamy, T.G. Mason, H. Gang, and D.A. Weitz, Phys. Rev. Lett. **76**, 3017 (1996).
[33] S. Cohen-Addad, H. Hoballah, and R. Höhler, Phys. Rev. E **57**, 6897 (1998).
[34] The model predicts that the application at $t' = 0$ of a larger step strain (out of the linear regime) leads to an effective aging exponent smaller than μ. We have not performed such experiments out of the linear regime. This prediction is, however, compatible with observations reported in Ref. [10] (cf. note [25]).